Molecular Crystals and Liquid Crystals
Publication details, including instructions for authors and subscription information:
http://www.tandfonline.com/loi/gmcl16

Factors Affecting the Anisotropic and Dynamic Scattering Characteristics of an Ester Mixture

J. David Margerum [a], Anna M. Lackner [a], Hong S. Lim [a] & John E. Jensen [a]
[a] Hughes Research Laboratories, 3011 Malibu Canyon Road Malibu, California, 90265, USA
Version of record first published: 20 Apr 2011.

To cite this article: J. David Margerum , Anna M. Lackner , Hong S. Lim & John E. Jensen (1984): Factors Affecting the Anisotropic and Dynamic Scattering Characteristics of an Ester Mixture, Molecular Crystals and Liquid Crystals, 111:1-2, 135-159

To link to this article: http://dx.doi.org/10.1080/00268948408082179

Mol. Cryst. Liq. Cryst. 1984, Vol. 111, pp. 135-159
0026-8941/84/1112-0135/$18.50/0

Printed in the United States of America

FACTORS AFFECTING THE ANISOTROPIC AND DYNAMIC SCATTERING CHARACTERISTICS OF AN ESTER MIXTURE

J. DAVID MARGERUM, ANNA M. LACKNER,
HONG S. LIM, AND JOHN E. JENSEN
Hughes Research Laboratories
3011 Malibu Canyon Road
Malibu, California 90265 USA

Various factors affecting the anisotropic and dynamic scattering (DS) characteristics of a 3-component eutectic mixture of phenyl benzoates are investigated in detail. The effects of dopant, surface alignment, signal, cell thickness, and temperature are studied. Different dopant structures give conductivity anisotropy values in the 1.01 to 1.60 range and this has the largest effect on the DS threshold voltage at room temperature. However, cell thickness also changed the threshold slightly and has a large effect on the magnitude of the scattering obtained above threshold. Thinner cells give higher DS levels, higher multiplexing capabilities, and greater off-angle scattering. The optical density of scattering increases linearly with the reciprocal of cell thickness. At elevated temperatures the conductivity anisotropy, viscosity and elastic constant values all decrease. However, with the increasing temperature the DS threshold voltage decreases, indicating that changes in viscosity and elastic constants with temperature are more significant than the decrease in conductivity anisotropy.

1. INTRODUCTION

We are interested in using the dynamic scattering (DS) mode[1] in liquid crystal (LC) devices such as pictorial matrix displays[2,3,4], reticle devices[5,6], and automobile dashboard displays[7]. Phenyl benzoate ester mixtures of negative dielectric anisotropy are of interest for DS, because they are colorless, can be purified adequately for controlled doping[8], show good dc stability when used with redox dopants[9,10] and have relatively good thermal stability at elevated temperatures[11]. In many of these applications it is desirable to have a low threshold voltage (V_{th}) for the DS mode. The present study is designed to evaluate, in detail, the factors affecting the V_{th} and scattering levels of a phenyl benzoate LC mixture. These factors include the conductivity dopant, resistivity, temperature, surface alignment, applied signal and cell thickness. A simple LC eutectic mixture (HRL-2N25) containing just three phenyl benzoate components is used for these studies, and its properties are also characterized as a function of temperature.

2. EXPERIMENTAL

Most of the experimental techniques employed here have been described[11,12]. The ester LC components are synthesized and purified by standard methods. Liquid chromatography

analysis indicates that these components have less than 0.1% impurity. The room temperature resistivity of the undoped LC mixture is greater than 10^{11} ohm-cm, typically about 4×10^{11} ohm-cm. The dopants are prepared in the following ways: Tetracyanoethylene (TCNE) from Aldrich is recrystallized from methylene chloride and then sublimed at 70°C. Tetrabutylammonium trifluoromethanesulfonate (TBATMS) is prepared as previously reported[8]. Ethylpyridinium tetraphenylboride (EPTPB) and tetrabutylammonium tetraphenylboride (TBATPB) are prepared in the manner described by Mann[13], with recrystallization from acetone/water solutions before drying. Dibutylferrocene (DBF) from Research Organic Chem. is distilled at 115°C at 0.3mm. (2,4,7 Trinitrofluorenylidene)-malononitrile (TFM) from Aldrich is recrystallized from acetonitrile. (2,4,5,7-Tetranitrofluorenylidene)malononitrile (T4FM) is synthesized by reacting 2,4,5,7-tetranitro-9-fluorenone with malononitrile; the reactants are from Aldrich, and the product is recrystallized from acetonitrile. Dodecyl-(ethyl)dimethylammonium p-hexyloxybenzoate (ZLI-235) is used as obtained from E. Merck.

The DS is measured[8] in transmission at normal incidence and the V_{th} is obtained by extrapolation back to the baseline of no scattering, using unpolarized green light centered at 525nm. In the scattering angle

measurements the light is incident normal to the cells, and the detector system is rotated off-normal. With no DS the light intensity reaching the detector is 1% of normal transmission intensity at ± 4.5°. Several different surface alignment techniques are used. Cells with surface-parallel LC alignment are made by rubbing ITO (indium tin oxide) electrode surfaces, or by rubbing a thin coating of polyvinyl alcohol (PVA) on ITO after drying in an oven, or by shallow angle ion beam etching of ITO, or by medium angle deposition (MAD) of SiO on ITO[14]. The surface-perpendicular LC alignment is made by bonding a long chain alcohol ($C_{18}H_{37}OH$) onto a thin (150Å) coating of MAD-SiO on ITO, except in the field effect measurements (no DS) where the C_{18} alcohol treatment is used on a SiO_2 (800 Å) coating in order to minimize the tilt angle[15]. Cell thickness variations are made using various Mylar films as perimeter spacers for normal thickness. The actual thickness of the thinner LC cells is calculated from the resistance measurements of each cell and the resistivity of each LC sample in thicker cells (50.8 or 127 μm). The width of the Williams domains[16] is measured with a Zeiss Standard WL polarizing microscope, using minimum applied voltages in the range of 1.04 to 1.23 times V_{th}.

3. RESULTS AND DISCUSSION

3.1 LC Eutectic Mixture

A three component eutectic ester mixture, identified as HRL-2N25, is formulated using p-ethoxyphenyl p-propylbenzoate (20-3), p-hexyloxyphenyl p-butylbenzoate (60-4), and p-hexyloxyphenyl p-methoxybenzoate (60-01) as shown in Table I. The ratio of components is calculated with the Schroeder-van Laar equation. The actual nematic range, observed by differential scanning calorimetry, has both a lower melting point and clearpoint than the calculated values. Several other properties of the mixture are also summarized in Table I, including the average molecular length (L) which is determined from measurements of molecular models in the extended configuration[12]. The dielectric anisotropy ($\Delta\varepsilon$) is more negative than mixtures of 100% RO-R' (e.g 20-3, 60-4, etc.) components[12] due to the RO-OR' (60-01) component. The capillary flow viscosity (η) is relatively high due to the medium size L and the presence of 60-01 as shown by other studies of RO-R'/RO-OR' mixtures[17]. The viscosity data fit the expression $\eta = A \exp(E_\eta/RT)$ quite well.

3.2 Dopants and Conductivity Anisotropy

Purified mixtures are usually not conductive and will show DS effects only if ionic species are

Table I. HRL-2N25 Eutectic Mixture

Component Code	L (Å)	mp (°C)	Clpt. (°C)	ΔH_f kcal/mole	Mole Fraction
20-3	19.67	76	68	6.72	.132
60-4	25.78	29	48	4.20	.640
60-01	23.60	55	80	6.19	.228

Properties

Calc. nematic range: 13° to 57°C

Obs. nematic range: 0° to 54°C

Av. molecular length: $\bar{L}$ = 24.48 Å

Dielectric anisotropy: $\Delta\varepsilon$ = -0.39 (24°C, 1kHz)

Birefringence: Δn = 0.14 (23°, 589nm)

Freedericks transition: V_{FT} = 7.0 V (23°C)

Density: d = 1.059 g/ml (25°C)

Flow viscosity: η = 48.5 cP (25°C)

Viscosity activation energy: E_η = 9.3 kcal/mole

present or are generated by the applied field. Both the ionic conductivity and its anisotropy depend upon the structure of dopant as well as the LC[8,18,19]. The seven dopants in this study are chosen to provide a wide range of conductivity anisotropy ($\sigma_\parallel/\sigma_\perp$) values. In this ester mixture the $\sigma_\parallel/\sigma_\perp$ of each dopant except TBATMS is nearly independent of concentration, as indicated in Figure 1. Except for EPTPB and T4FM, these dopants have been studied in various other LCs and similar results are found here. In HRL-2N25 at 25°C the $\sigma_\parallel/\sigma_\perp$ value is 4 to 6% higher for TBATMS, TBATPB, and DBF/TFM than in

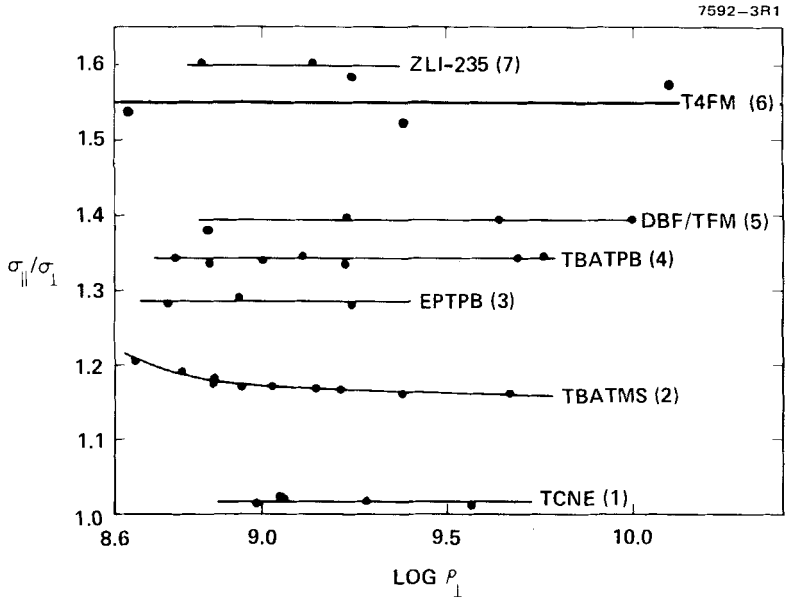

FIGURE 1 Conductivity anisotropy of dopants in HRL-2N25 at 23°C as a function of resistivity ($\rho_\perp$ at 100 Hz).

the HRL-2N10 ester mixture[8], is 5% lower for ZLI-235 than in a Schiff base-ester mixture[20], and is 3% lower than TCNE in an azoxy LC[21]. Although changes in the dopant structure often have a larger effect on the conductivity anisotropy of nematic mixtures than changes in the LC structure, much larger variations of $\sigma_\parallel/\sigma_\perp$ are observed in other LC mixtures in which cybotactic nematic characteristics are present[11,12,22].

3.3. Effects of Dopant, Alignment, and Frequency on V_{th}

Figure 2 shows plots of V_{th} for ac-DS (30 Hz for both surface-perpendicular and surface-parallel cells) and for dc-DS (surface-parallel), each as a function of the conductivity anisotropy of the seven dopants in HRL-2N25. The dopants are identified by the number indicated in Figure 1. In these samples the DS cutoff frequency is greater than 250 Hz, so that approximately constant V_{th} values are observed for dopants 2-7 in the 10-30 Hz range. In dopant 1 (TCNE) the value of V_{th} is progressively lower in going from 30 Hz to 20 Hz and to 10 Hz, indicating that in this case some electrochemical reactions are lowering the V_{th} value at the low frequencies. The conductivity anisotropy has a very large effect on V_{th} in both types of surface alignments and with dc-DS as well as ac-DS. (The dc-DS measurements are less reproducible, but typical V_{th} values are shown here. The relatively high dc-V_{th} for dopant 7 may be due partly to its strong tendency to cause surface- alignment). For a given dopant the DS thresholds here follow the pattern: ac-$V_{th}(\perp)$ > ac-$V_{th}(\parallel)$ > dc-$V_{th}(\parallel)$. This supports earlier observations discussed regarding other LC/dopant systems[23]. Charge injection effects[10] appear to play a dominant role in the dc-activated cells. In contrast to ac-activation, the microscopic patterns of the instability under dc-activation vary with the

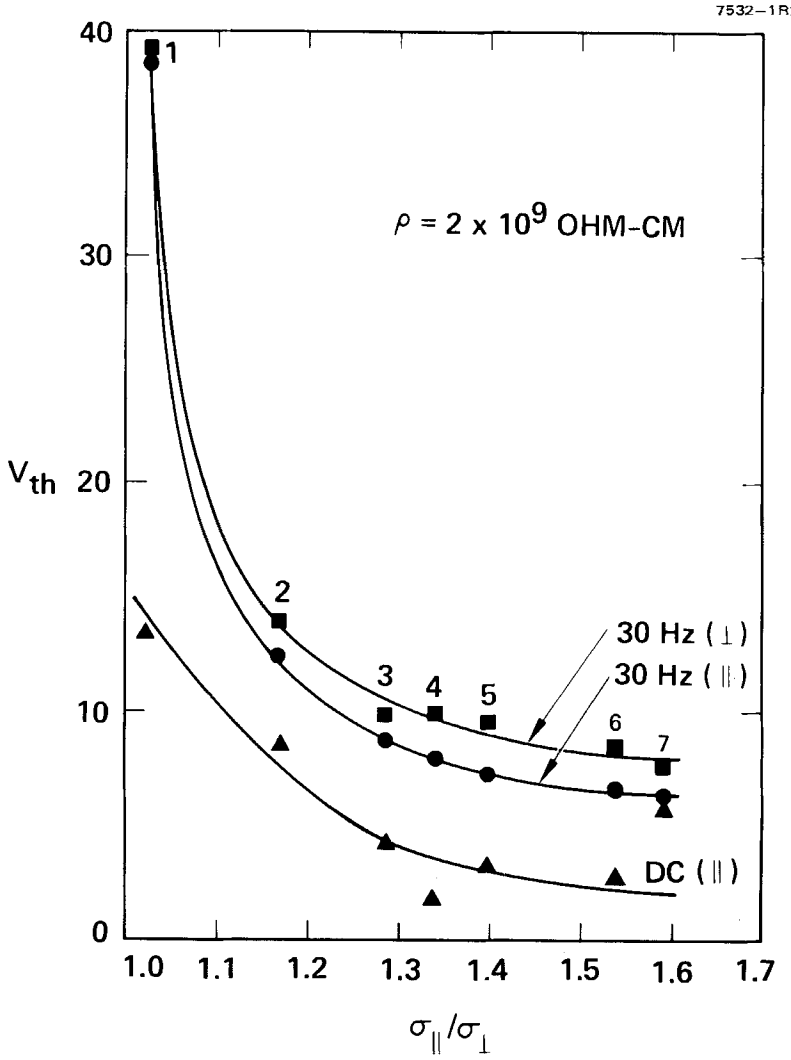

FIGURE 2 Dynamic scattering threshold voltage as a function of the conductivity anisotropy and surface alignment of HRL-2N25 containing the dopants in Table 1. (23°C, $\rho_{\perp} = 2 \times 10^9$ Ω-cm, ■-surface-⊥, ● and ▲-surface-∥).

individual dopants. The general appearance of these patterns are similar to a wallpaper pattern while the ac-activated Williams domains consist of many parallel line domains. The dc-V_{th} decreases with increasing $\sigma_{\parallel}/\sigma_{\perp}$, but the values do not fit the correlation derived by Helfrich[24] for the Williams domain threshold variation with $\sigma_{\parallel}/\sigma_{\perp}$, even though the expression was derived for dc fields. It should be noted that the values of conductivity anisotropy are obtained with ac measurements at 100 Hz. This gives the $\sigma_{\parallel}/\sigma_{\perp}$ for the ionic species present in the bulk of the LC from the dopant under equilibrium conditions. It does not measure the conductivity anisotropy of electrochemically generated ionic species which are formed by dc activation, and such ions could have a larger anisotropy than the initial dopants. This is the case for T4FM, whose V_{th} values (both ac and dc) decrease after periods of dc-activation. If the ionic transport in the dc cells is carried by both dopant ions and dc-generated ions of higher conductivity anisotropy, then this could explain the observed dc results.

The qualitative expressions derived by Helfrich[24] for the V_{th} of Williams domains (corresponding here to the ac-V_{th} of DS) indicate that the correlations shown in equations 1 and 2 should be followed if small amounts of conductivity dopants in HRL-2N25 change only its $\sigma_{\parallel}/\sigma_{\perp}$, and do not affect the

values of A, B, C and D.

$$\bullet \text{ Surface-}\parallel : \quad V_{th}^{-2} = A\left(\frac{\sigma_\parallel}{\sigma_\perp}\right)^{-1} + B \quad , \tag{1}$$

where, $A = \dfrac{1}{4\pi^3 k_{33}}\left(\Delta\epsilon - \dfrac{K_1\epsilon_\parallel}{\eta_1}\right)$; $\quad B = \dfrac{K_1\epsilon_\perp}{4\pi^3 k_{33}\eta_1}$

$$\bullet \text{ Surface-}\perp : \quad V_{th}^{-2} = C\left(\frac{\sigma_\parallel}{\sigma_\perp}\right) + D \quad , \tag{2}$$

where, $C = \dfrac{-1}{4\pi^3 k_{11}}\left(\Delta\epsilon + \dfrac{K_2\epsilon_\perp}{\eta_2}\right)$; $\quad D = \dfrac{K_2\epsilon_\parallel}{4\pi^3 k_{11}\eta_2}$

The expressions of V_{th} with ac activation[25,26] contain extra terms of frequency dependence. However, these terms drop out if the frequency applied is substantially below the cut-off frequency, which is the case in the present studies. Using the ac data from Figure 2, there is a good fit of the surface-parallel data with Equation 1, and of the surface-perpendicular data with Equation 2, as shown by the least-square plots in Figure 3. These results indicate that in each of these surface alignment boundary conditions the effects of various dopants on the ac-V_{th} is determined largely by the conductivity anisotropy of the dopant in the LC.

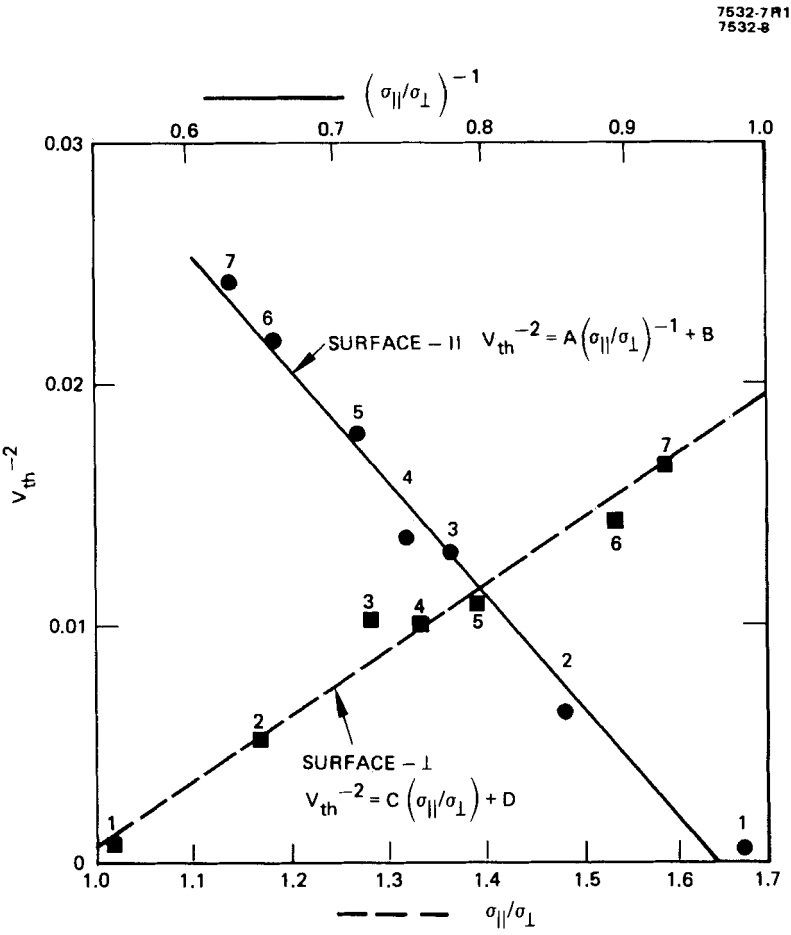

FIGURE 3 Helfrich equation plots for surface-dependence of ac dynamic scattering V_{th} on $\sigma_{\parallel} / \sigma_{\perp}$

3.4 Effects of Resistivity on V_{th}

Some effects of LC resistivity (ρ) on the ac and dc values of V_{th} are shown in Figure 4 for

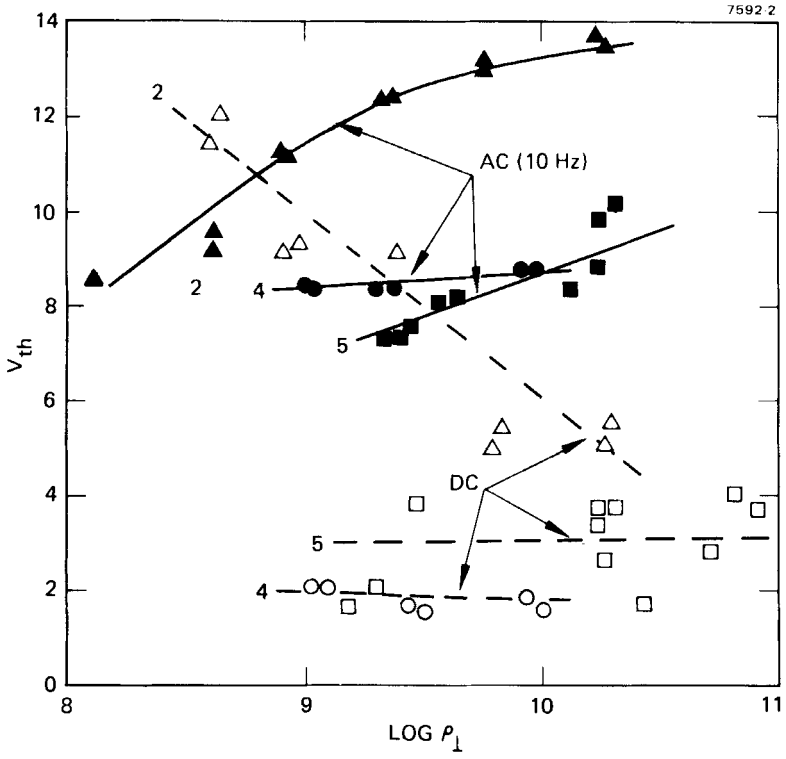

FIGURE 4 Effect of resistivity ($\rho_\perp$ at 100 Hz) on dynamic scattering V_{th} of doped HRL-2N25 in 12.7 μm thick cells with surface-$\parallel$ alignment, rubbed ITO.

○,● - TBATPB (4); △,▲ - TBATMS (2); □,■ - DBF/TFM (5).

dopants 2, 4, and 5. In each case the ac-V_{th} increases as ρ increases. In the TBATMS samples, the change in ac-V_{th} is partially accounted for by the changes of its conductivity anisotropy with $\rho_\perp$ which are shown in Figure 1. However, since the $\sigma_\parallel/\sigma_\perp$ values of TBATPB and

DBF/TFM are constant with ρ some other (unknown) factor causes their V_{th} to change with ρ. The dc-V_{th} effects vary with the electrochemical properties of the dopants. The dc-V_{th} of TBATMS-doped samples decreases markedly as ρ increases. This dopant is more electrochemically stable than the LC, and the LC probably reacts under a dc field to give LC^+ and LC^- species[9,10] which may have relatively high conductivity anisotropy. At a ρ of 10^9 ohm-cm the LC contains about 10^{-4}M TBATMS, giving an ionic concentration of approximately 10^{-5}M. As the ionic concentration is decreased, the concentration of the positive ions in the vicinity of the positive electrode and of the negative ions in the vicinity of the negative electrode will be decreased as a result of coulombic interaction. Thus dc generated LC ions would be expected to contribute to the ionic transport current, and this becomes more significant as ρ is increased. The ρ of the TBATMS-doped cells under continuous dc-DS decreases significantly only after hours of activation[9], presumably due to irreversible reactions of the LC^+ and LC^- species. On the other hand, the ρ of TBATPB-doped samples changes fairly rapidly (in 10 minutes) with dc-activation, indicating that the dopant itself reacts readily and irreversibly at the electrodes. These reactions of TBATPB appear to result in species of high $\sigma_{\parallel}/\sigma_{\perp}$, giving low dc-

V_{th} values for the short lifetime period of the samples. The DBF/TFM dopant pair is a redox system chosen to protect the LC by reacting readily and reversibly at the electrodes[9,10]. For a ρ of 10^9 ohm-cm the neutral DBF and TFM compounds are each added in about 3×10^{-2}M, so that there are larger concentrations of these redox dopants present than in the case with the salt dopants. Because of their electrochemical stability and the amounts of DBF and TFM present, the dc-V_{th} is relatively stable for very long periods of dc activation. The variations of dc-V_{th} for DBF/TFM in Figure 4 may be due to some differences in the surface adsorption of these dopants on the electrodes.

3.5 Effects of Cell Thickness

The ac-V_{th} of DS is not constant with the thickness of the cell, as shown by the upper plot in Figure 5. There is a V_{th} minimum at thicknesses of approximately 25 μm. In thicker cells the V_{th} increases appreciably, possibly due to the increase in the ℓ/λ term as shown by equation 3 and the lower curve in Figure 5 (where ℓ is the

$$V_{th} = \pi \left(\frac{2\ell}{\lambda}\right) \left[\frac{k_{33}/\epsilon_o}{\frac{\kappa_1 \epsilon_\parallel}{\eta_1} \left(\frac{\epsilon_\perp}{\epsilon_\parallel} - \frac{1}{R_o}\right) + \frac{\Delta\epsilon}{R_o}} \right]^{1/2} \qquad (3)$$

cell thickness and λ is the Williams domain periodicity). However, in cells thinner than

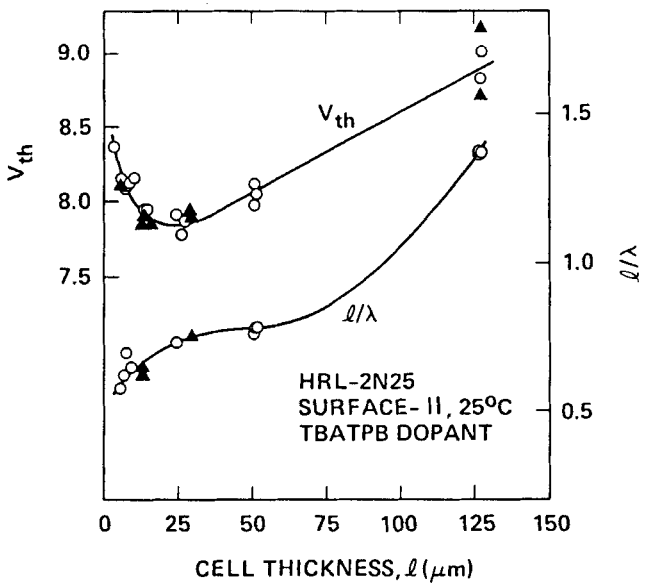

FIGURE 5 Effect of cell thickness on DS-V_{th} and on domain periodicity (λ), 30Hz.
○ rubbed PVA on ITO
▲ rubbed ITO, or ion-beam etched ITO

25 μm the V_{th} also increases while the ℓ/λ term decreases. We do not know the reason for the increased V_{th} in thin cells. Cells with and without PVA coatings for surface-|| alignment gave the same results, so the effect does not appear to be an artifact related to a voltage drop across the PVA. Also the resistivity changes have little effect in the range used with ρ between 6.15×10^8 and 1.36×10^9 ohm-cm.

The scattering level of DS (where % S = 100 - % T, for cells measured in transmission with light at normal incidence) is

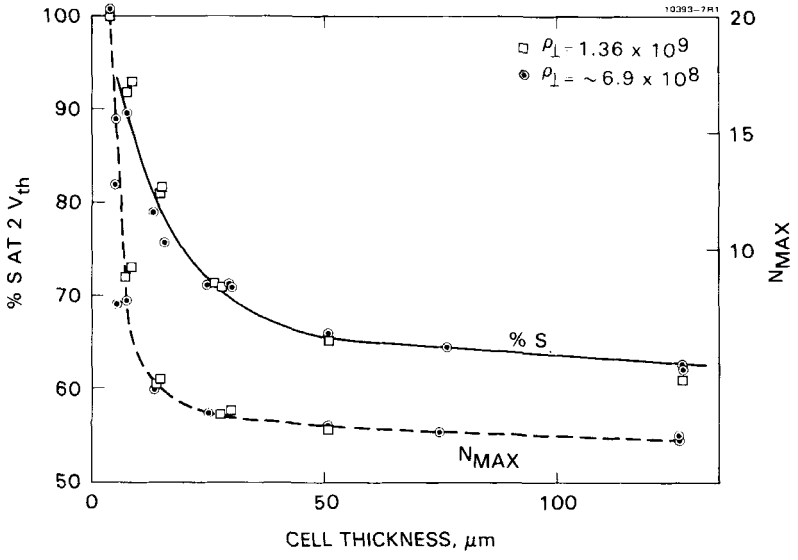

FIGURE 6 The effect of cell thickness on %S and on N_{max} at 70%S (23°C).

higher in thinner cells. This is shown in Figure 6, where the % S is plotted versus cell thickness at 2 x V_{th} for each thickness. The % S increases sharply in thin cells (we did not use cells thin enough to observe the expected decrease in very thin cells). We find a linear relationship between the optical density of scattering and the reciprocal of the cell thickness as shown in Figure 7. In Figures 6 and 7 the maximum multiplexing capability[27] (N_{max}) for 70% S is also shown. The N_{max} increases greatly in thin cells, which of course also have the advantages of having much faster response times.

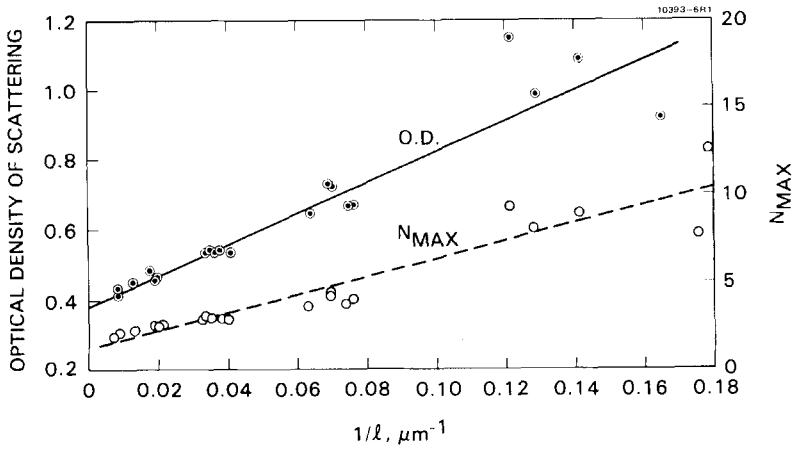

FIGURE 7 Reciprocal length plots for the optical density of scattering (-log T) and the maximum multiplex capability.

The data in Figures 6 and 7 are from measurements made with normal incident light scattered by DS at relatively small off-angles (about ± 4°). The effect of cell thickness on light scattered at larger off-angles is also examined. As shown in Figure 8, the intensity of off-angle scattered light in the 4-15° range is higher for a thin cell than for thicker cells. (Here the relative intensities are given as the values measured at 2 x V_{th} divided by the intensity at that angle from a one-half Lambertian plate.) Thus, the results from Figure 8 indicate that the DS efficiency of thin cells is superior to that of thick cells for light scattered at larger (4-15°) angles as well as at small angles.

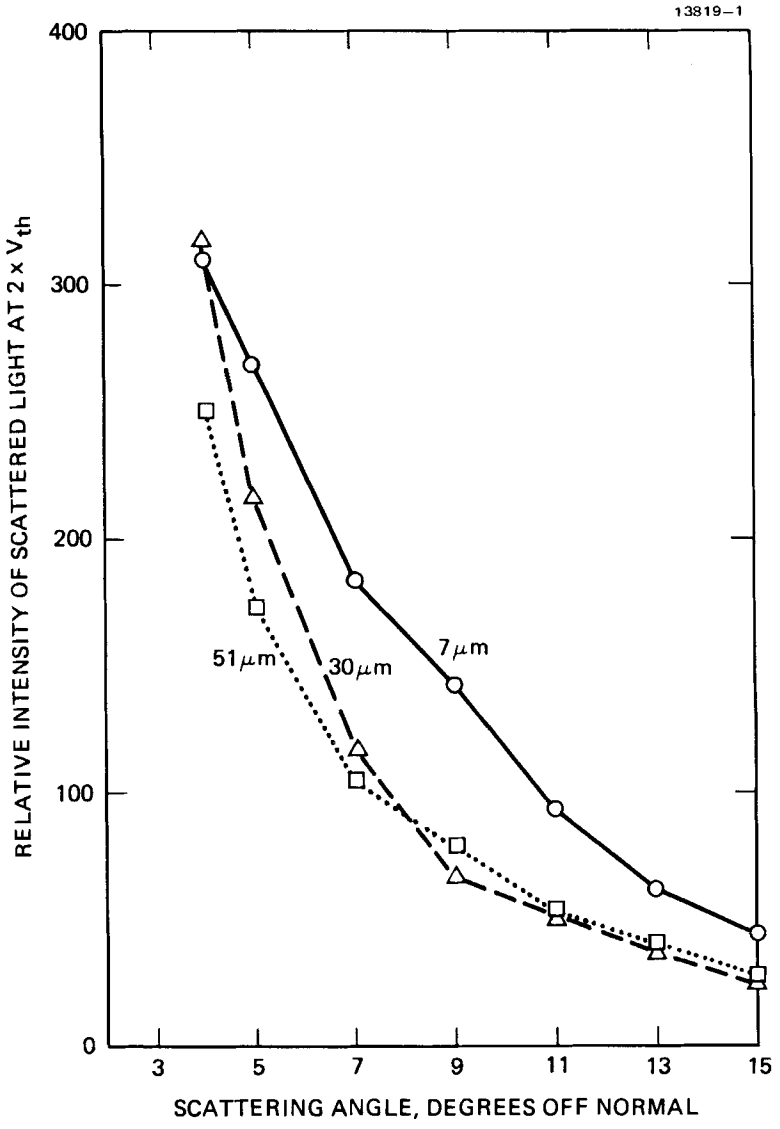

FIGURE 8 Cell thickness effect on off-angle DS intensity.

3.6 Temperature Effects

The effects of temperature on several anisotropic and electro-optical properties of HRL-2N25 are shown in Figures 9 and 10. The Freedericks transition in Figure 9 refers to the field effect threshold in a surface-$_{\perp}$ cell. The values of $(V_{th}')_{FT}$ and $\Delta\varepsilon$ in Figure 9 are used to calculate the k_{33} elastic constant shown in Figure 10. The $\sigma_{\parallel}/\sigma_{\perp}$ and V_{th} values of DS are measured using TBATPB as a conductivity dopant. The most interesting result in Figure 10 is that the DS-V_{th} values decrease with increasing temperature (at least up to 50°C) while the $\sigma_{\parallel}/\sigma_{\perp}$ also decrease in the same temperature range. This is surprising considering the large effect that $\sigma_{\parallel}/\sigma_{\perp}$ has on the V_{th} (see Figure 2). It indicates that the temperature effects on other parameters such as elastic constants and viscosity coefficients are large enough and in the opposite direction, to offset the decrease of $\sigma_{\parallel}/\sigma_{\perp}$. This is consistant with the large decreases observed in k_{33} and η with increasing temperature.

4. CONCLUSIONS

In brief, our studies with this phenyl benzoate LC mixture show the following correlations:

1. The V_{th} for DS is strongly affected by the choice of conductivity dopant, LC surface alignment, and the applied voltage frequency.

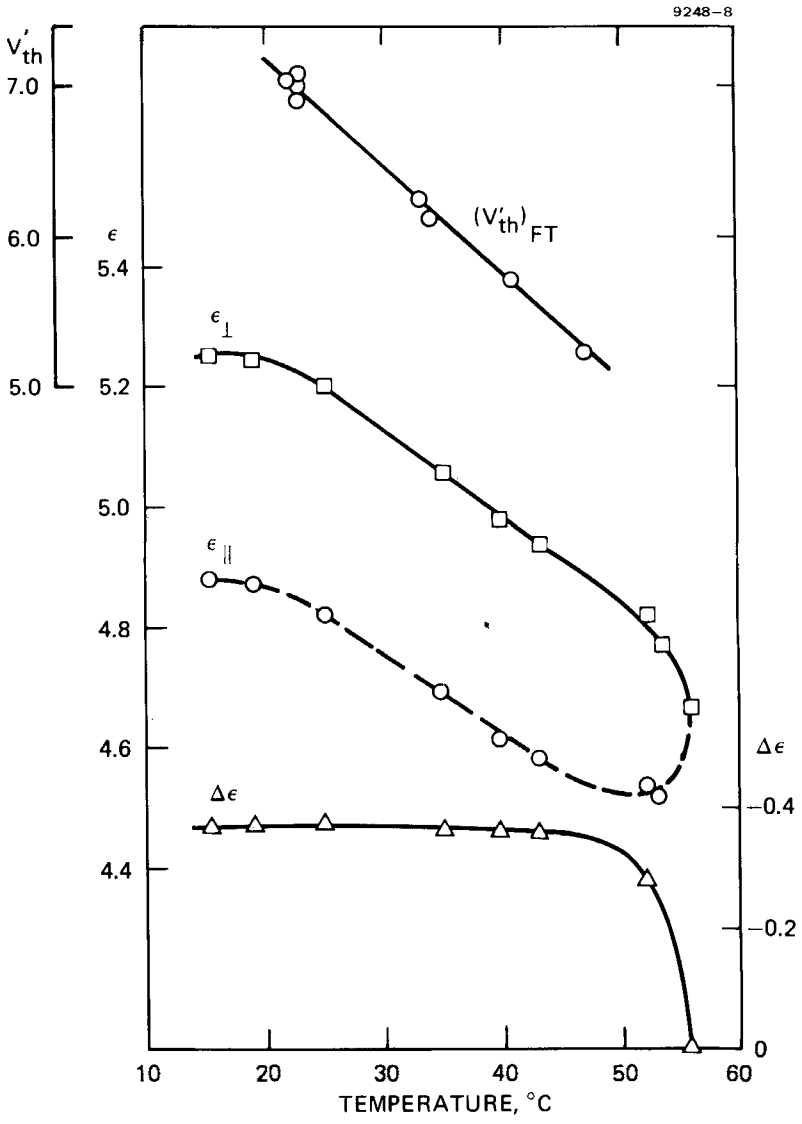

FIGURE 9 Temperature effects on dielectric properties and Freedericks transition of HRL-2N25 (undoped).

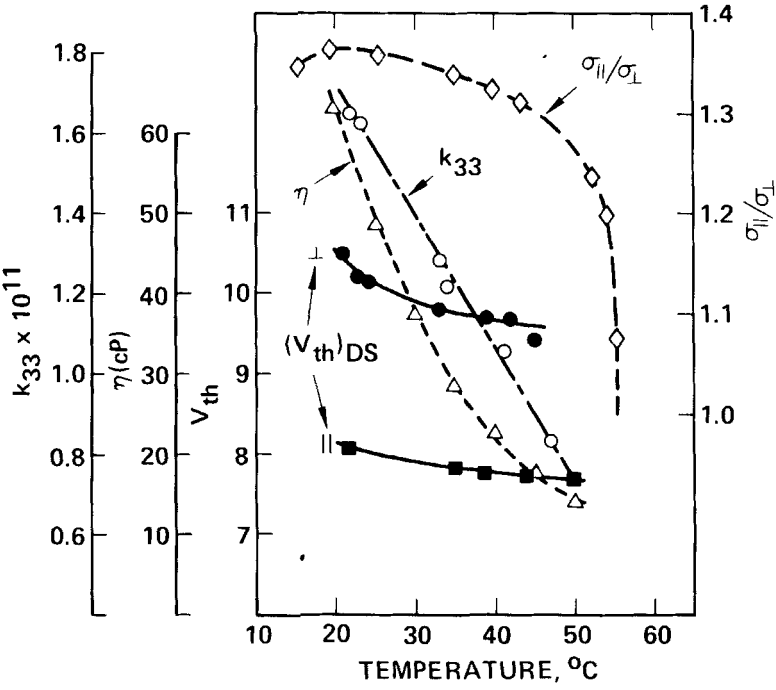

FIGURE 10 Temperature effects on properties of HRL-2N25, with TBATPB dopant.

The effect of dopant conductivity anisotropy on V_{th} is well correlated over a wide range by Helfrich's equations for both surface-parallel and surface-perpendicular LC alignment at low ac frequencies. A similar trend is observed with dc signals, but the correlation is obscured by electrochemical effects. In general, the lowest V_{th} values are obtained with high conductivity anisotropy, surface-parallel alignment, and dc signals.

2. In this LC the V_{th} is also affected by the LC resistivity, cell thickness, and temperature. Smaller ac-V_{th} values are obtained with lower resistivity, with a cell thickness of about 25 μm, and at higher temperatures up to about 50°C. At these elevated temperatures the V_{th} is less affected by the decrease in conductivity anisotropy than by the offsetting decreases in the elastic constant and viscosity of the LC.

3. When compared at an applied voltage of $2 \times V_{th}$, thinner cells show higher scattering levels, higher multiplexing capability and more off-angle scattering than thicker cells. Both the "optical density" of scattering and the maximum multiplexing capability increase linearily with the reciprocal of the cell thickness.

5. ACKNOWLEDGMENTS

This work was supported in part by the Directorate of Chemical Sciences, Air Force Office of Scientific Research Contract F49620-77-C-0017, and by the Office of Naval Research. We are also indebted to W. H. Smith, Jr. for assistance in the DSC measurements, and to C. S. Bak for setting up the off-angle scattering apparatus.

REFERENCES

1. F. G. HEILMEIER, L. A. ZANNONI, and L. A. BARTON, Proc. IEEE, 56, 1162 (1968).
2. M. H. ERNSTOFF, A. M. LEUPP, M. J. LITTLE, and H. T. PETERSON, IEEE Electron Device Conf. Digest, Washington, D. C. (Dec. 1973).
3. J. D. MARGERUM and L. J. MILLER, J. Colloid and Interface Sci., 58, 559 (1977).
4. M. YOSHIYAMA, T. MATSUO, K. KAWASAKI, H. TATSUTA, and T. ISHIHARA, 8th Int'l Liq. Cryst. Conf., paper I-14, Kyoto, Japan (July 1980).
5. C. H. GOOCH, R. BOTTOMLEY, J. J. LOW, and H. A. TARRY, J. Phys. E, 6, 485 (1973).
6. R. P. FARNSWORTH, L. W. HILL, and S.-Y. WONG, U. S. Patent 3,885,861 (May 27, 1975).
7. Y. OHSAWA, T. FUJII, Y. OKADA, and S. KANABE, 8th Int'l Cryst Conf., Paper I-26P, Kyoto, Japan (July 1980).
8. J. D. MARGERUM, H. S. LIM, P. O. BRAATZ, and A. M. LACKNER, Mol. Cryst, Liq. Cryst., 38, 219 (1977).
9. H. S. LIM and J. D. MARGERUM, Appl. Phys Lett., 28, 478 (1976).
10. H. S. LIM, J. D. MARGERUM, and A. GRAUBE, J. Electrochem. Soc. 124, 1389 (1977).
11. J. D. MARGERUM and A. M. LACKNER, Mol. Cryst. Liq. Cryst., 76, 211 (1981).
12. J. D. MARGERUM, J. E. JENSEN, and A. M. LACKNER, Mol. Cryst. Liq. Cryst., 68, 137 (1981).
13. C. K. MANN, Electroanalytical Chemistry, A. J. Bard, ed. (Marcel Dekker, N. Y. 1969), 3, p. 132.
14. J. L. JANNING, Appl. Phys. Lett 21, 173 (1972).
15. L. J. MILLER, J. GRINBERG, G. D. MYER, D. S. SMYTHE, and W. S. SMITH, Liquid Crystals and Ordered Fluids, J. E. Johnson and R. S. Porter, eds. (Plenum Press, 1978), 3, p. 513.

16. R. WILLIAMS, J. Chem. Phys., 39, 384 (1963).
17. J. D. MARGERUM, S.-M. WONG, J. E. JENSEN and C. I. VAN AST, Liq. Cryst. and Ordered Fluids, A. C. Griffin and J. E. Johnson, Ed. (Plenum Press, 1984), 4, p. 111.
18. R. CHANG, Liquid Crystals and Ordered Fluids, J. E. Johnson and R. S. Porter, Ed. (Plenum Press, 1974), 2, p. 367.
19. M. I. BARNIK, L. M. BLINOV, M. F. GREBENKIS, S. A. PINKIN, and V. G. CHIGRINOV, Physics Letters, 51A, 175 (1975).
20. G. HEPPKE, F. SCHNEIDER, Z. Naturforsch, 31A, 611-14, (1976).
21. M. I. BARNIK et al., Sov. Phys - JETP 42, 550 (1976), Zh Eksp. Teor. Fiz. 69, 1080 (1975).
22. J. D. MARGERUM, S.-M. WONG, A. M. LACKNER, and J. E. JENSEN, Mol. Cryst. Liq. Cryst. 68, 157 (1981).
23. M. J. LITTLE, H. S. LIM, and J. D. MARGERUM, Mol. Cryst. Liq. Cryst, 38, 207 (1977).
24. W. HELFRICH, J. Chem. Phys., 51, 4092 (1969).
25. ORSAY LIQUID CRYSTAL GROUP,(a) Phys. Rev. Lett., 25, 1642 (1970); (b) Mol. Cryst. Liq. Cryst., 12, 251 (1971).
26. E. DUBOIS-VIOLELLE, P. G. DEGENNES and O. PARODI, J. Physique, 32, 305 (1971).
27. P. M. ALT and P. PLESHKO, IEEE Trans. Electron Devices, ED-21, 146 (1974).